Polymer 49 (2008) 2560–2567

Contents lists available at ScienceDirect

Polymer

journal homepage: www.elsevier.com/locate/polymer

# Biaxial stress–strain behavior of chemical and physical gels of poly(vinyl alcohol)

Bohumil Meissner*, Libor Matějka

*Institute of Macromolecular Chemistry, Academy of Sciences of the Czech Republic, Heyrovský Square 2, 162 06 Prague 6, Břevnov, Czech Republic*

ARTICLE INFO

*Article history:*
Received 30 January 2008
Received in revised form 31 March 2008
Accepted 2 April 2008
Available online 8 April 2008

*Keywords:*
Poly(vinyl alcohol) gels
Pure shear behavior
Constitutive equation

ABSTRACT

In a recent paper, Urayama K, Ogasawara S, Takigawa T [Polymer 2006;47:6868–73.] found significant differences in the pure shear behavior of the poly(vinyl alcohol) gels with similar initial modulus but with different types of crosslinks, physical crosslinks formed by microcrystallites and chemical crosslinks made of covalent bonds. The non-Gaussian three-chain model was found to give but a limited explanation of the data. In this paper we show that the constitutive equation that we proposed and tested previously (Polymer 2006) for filler-reinforced rubber networks gives equally good description and reasonable interpretation of the stress–strain data on poly(vinyl alcohol) gels in different geometrical modes. The Arruda–Boyce eight-chain model combined with the Gaylord–Douglas theory of tube-like topological constraints describes well the stress–strain properties of chemical gels in pure shear and in uniaxial and equibiaxial extensions. The pure shear behavior of physical gels can be reasonably explained and described by taking into account the amplification of local strain in the presence of inextensible particles (crystalline domains).



## 1. Introduction

In a recent paper, Urayama et al. [1] have investigated the stress–strain properties of physical and chemical gels of poly(vinyl alcohol) (PVA). The physical gels were prepared by cooling PVA solutions (12 and 15 wt%) in a mixture of dimethyl sulfoxide and water (4:1) for 24 h at −20 °C. Under such conditions, crystallization takes place and the network junctions of the resulting gels are formed by PVA microcrystallites. The chemical gels were prepared by crosslinking water solutions of PVA (7.5, 10, 12 wt%) with glutaraldehyde. The stress–strain properties of the gels were measured in three different modes of deformation: uniaxial extension (UE), equibiaxial extension (EBE) and pure shear (PS). The authors compared the ratio $R = \sigma_1/\sigma_2$ of the principal pure shear stresses, longitudinal $\sigma_1$ (sPS1) and transverse $\sigma_2$ (sPS2), with theoretical predictions and found that the simple non-Gaussian elasticity theory based on the three-chain network model of James and Guth [2,3] predicted the stretch ratio ($\lambda_1$) dependence of $R$ measured on physical gels reasonably well. While in physical gels the ratio $R$ was found to increase with stretch ratio at a higher rate than predicted by the Gaussian rubber elasticity theory, in chemical gels it was lower than the Gaussian prediction and almost independent of stretch ratio. The authors state that such effect is not predicted theoretically. They concluded that none of the existing theories of rubber elasticity theory was able to fully describe the stress–strain behavior of PVA gels in all the four deformation modes studied.

In our opinion, the cited conclusion should possibly be expressed in a less general way: none of the existing theories based on models of freely penetrating volume-less chains is able to fully describe the stress–strain data of Urayama et al. The situation looks more hopeful if the experimental behavior is assessed in the light of theoretical approaches modeling not only the conformational elasticity of volume-less chains, but also other structural features contributing to the rubbery-elastic behavior, namely the impenetrability of real polymer chains [4–11] and the inextensibility of hard particles (fillers, crystalline or glassy domains) if they are present in the network [4,12].

Urayama et al. argue that in their chemical gels, even though the polymer concentrations in water are rather low, trapped chain entanglements are present and contribute to the network density [1]. The presence of entanglements suggests the impenetrability and non-zero volume of network chains; such features are modeled by tube theories [4–11]. They were shown to result in topological constraints on segment fluctuation and their contribution to the free energy and to stress has been calculated.

In physical PVA gels, microcrystallites play the role of network junctions. The crystalline domains have a much higher modulus than the rubbery matrix itself; they are practically inextensible in comparison with the matrix. The resulting hydrodynamic effects

* Corresponding author. Tel.: +420 296 809 384; fax: +420 296 809 410.
*E-mail addresses:* meissner@imc.cas.cz (B. Meissner), matejka@imc.cas.cz (L. Matějka).

0032-3861/$ – see front matter © 2008 Elsevier Ltd. All rights reserved.
doi:10.1016/j.polymer.2008.04.004

associated with the amplification of the local strain have been treated theoretically [4,12] and the relevant equations were successfully applied to filler-reinforced networks [13].

This paper shows that, with help of the mentioned theories and concepts, most features of the stress–strain behavior of PVA gels observed by Urayama et al. can be fairly well described and reasonably interpreted.

## 2. The Arruda–Boyce equation and the concept of a strain-dependent finite extensibility parameter

Arruda and Boyce used an eight-chain network model of volume-less chains and their result [14] for the principal (engineering) stresses $\sigma_i$ ($i = 1, 2$) (with $\sigma_3 = 0$) can be written in the form [13]:

$$\sigma_i = 2C_1 \frac{1 - (\lambda_c/\lambda_{cm})^2/3}{1 - (\lambda_c/\lambda_{cm})^2} \left(\lambda_i^2 - \lambda_3^2\right) \Big/ \lambda_i \quad (1)$$

$$I_1 = \sum_{i=1}^{3} \lambda_i^2;\ l_c = (I_1/3)^{1/2};\ \lambda_{cm} = N^{1/2} \quad (1a)$$

where $\lambda_i$ ($i = 1, 2, 3$) are the principal stretch ratios. The inverse Langevin function in the original equation of Arruda and Boyce is replaced here with the Padé approximation [15] in the same way as used previously [13]. The symbol for the theoretical shear modulus given in the original paper [14], $G_{th} = \nu RT$ ($\nu$ is the network-chain density), is replaced here with $2C_1$; $\lambda_c$ is the network-chain stretch ratio, i.e., the ratio of the deformed and undeformed chain end-to-end distances; $I_1$ is the first invariant of the deformation tensor (see Appendix A); $\lambda_{cm}$ is the hypothetical highest possible network-chain stretch ratio (or finite extensibility parameter, locking chain stretch ratio), which is predicted by the theory to be equal to the square root, $N^{1/2}$, of the network-chain length, with $N$ given by the number of statistical segments in the network chain (Eq. (1a)). For very long chains, $\lambda_{cm} \to \infty$, Eq. (1) reduces to the result of the Gaussian theory. The modulus $2C_1$ contains contributions both from chemical crosslinks and from trapped entanglements of the 'stable', i.e., junction-like nature [16]. The network-chain length, $N$, also seems to be determined by network junctions of both types.

Theories of the equilibrium rubber elasticity should be tested experimentally by comparing their predictions with reproducible and repeatable stress–strain dependences. The necessity of conditioning the network by prestraining to obtain a stabilized network structure and, as a result, reproducible biaxial data was shown, e.g., by James et al. [17,18]. In our previous paper we have found that prestrained networks (e.g., that of unfilled SBR) conform to the high-strain predictions of the Langevin-type theories very well [13] while the behavior of virgin networks at high strains is more complex [13,16,19,20].

It is instructive to compare the Arruda–Boyce equation (Eq. (1)) with the uniaxial stress–stretch ratio behavior of one of the hydrogel-type materials (Ref. [21], network DMAA–NC2.5–M1; here it is denoted by the code NC) that have been widely investigated in the last years by the Haraguchi group [21–23]. The polymer (poly(*N*,*N*-dimethylacrylamide), PDMAA) concentration in the hydrogel water is low (~10 wt%), the concentration of hard-phase nanoparticles (Mg–Li–Na silicate, Laponite XLG), which play the role of multifunctional crosslinks, is also low (~2 wt%) and the network chains, which are anchored to clay particles through their ends, are long, their molar mass $M_c$ being of the order of $10^2$ kg/mol. The deformation properties of such diluted networks might be expected to approach predictions of Eq. (1); however, this is not the case. The comparison of experiment–theory is shown in Fig. 1, where the experimental stretch ratio dependence of the stress in uniaxial extension (points) is plotted. Curves a and b, which are drawn using constant values of the finite extensibility parameter (see Table 1), are not able to satisfactorily describe the experimental data found on a virgin (previously unstrained) network, the stress of which increases at high stretch ratios at a lower rate than expected from the extrapolation of the curve a fitted to lower-strain data. Such behavior was observed previously on virgin unfilled and filler-reinforced rubber networks [13,16,19].

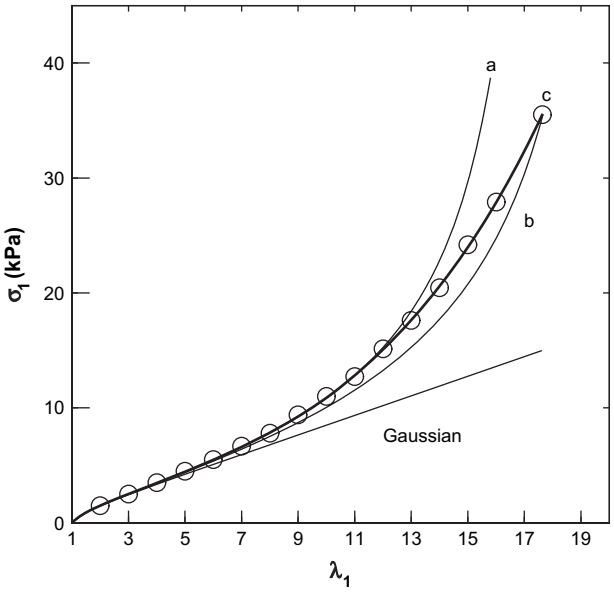


**Fig. 1.** Stress–strain dependence in UE determined on the NC hydrogel based on poly(*N*,*N*-dimethylacrylamide) and nanoplatelets of Mg–Li–Na silicate Laponite XLG. Experimental points are taken from Ref. [21, Fig. 7]. Curves a and b are drawn according to Eq. (1), curve c according to Eq. (1) with $\lambda_{cm}$ calculated according to Eq. (2); parameters are given in Table 1.

The reason for the more complex behavior of virgin networks was discussed previously [13,16,19]. It was interpreted as a relaxation effect which may be ascribed to some kind of strain-induced reorganisation of the network topology, its extent increasing with stretch ratio. A possible mechanism was proposed: trapped entanglements contributing to $C_1$ – in spite of behaving as stable network junctions at low and medium strains – may be forced by the increasing stress to slip along the network chains, in principle up to the nearest crosslinks. This would result in an increase in the network mesh size and lead to an increase in the finite extensibility parameter whose effect would partly persist on retraction and on second and subsequent extensions. The possibility of a strain-induced increase in the networks' mesh size on first stretching was anticipated in the literature (Wu and van der Giessen [20]) but so far no theoretical treatment of the effect was proposed.

The dependence of the finite extensibility parameter $\lambda_{cm}$ on the chain stretch ratio $\lambda_c$ of a given virgin network can be found by comparison of its experimental stress–strain dependence with

**Table 1**
Parameters of Eqs. (1) and (2) for curves in Fig. 1

| Parameter | Curves | | | |
|---|---|---|---|---|
| | Gaussian | a | b | c |
| $2C_1$ (kPa) | 0.85 | 0.85 | 0.85 | 0.85 |
| $\lambda_{c,a}$ | | | | 6.45 |
| $\lambda_{cm,a}$ | | | | 10.62 |
| $\lambda_{c,b}$ | | | | 10.215 |
| $\lambda_{cm,b}$ | ∞ [a] | 10.62[a] | 12.44[a] | 12.44 |
| $a$ | | | | 1.40 |

Network NC (hydrogel PDMAA/nanoclay).
[a] $\lambda_{cm}$.

Eq. (1) and can be described using the following empirical power function [19]:

$$\lambda_c \le \lambda_{c,a}, \quad \lambda_{cm} = \lambda_{cm,a}$$
$$\lambda_c > \lambda_{c,a}, \quad \lambda_{cm} = \lambda_{cm,a} + (\lambda_{cm,b} - \lambda_{cm,a})\left[(\lambda_c - \lambda_{c,a})/(\lambda_{c,b} - \lambda_{c,a})\right]^a \tag{2}$$

For chain stretch ratios lower than $\lambda_{c,a}$, the finite extensibility parameter is constant and equals to $\lambda_{cm,a}$. For chain stretch ratios higher than $\lambda_{c,a}$, attained not far above the inflection point of the stress–strain curve, the finite extensibility parameter begins to increase with strain and at the chain stretch ratio $\lambda_{c,b}$ it attains the value $\lambda_{cm,b}$. Curve c in Fig. 1 is drawn with $\lambda_{cm}$ increasing from 10.62 to 12.44 (see Table 1). The chain stretch ratio $\lambda_{c,b}$ corresponds to the highest stretch ratio used in the given experiment; sometimes the sample is stretched up to the break. Thus, $\lambda_{c,b}$ is not an adjustable parameter and $\lambda_{cm,b}$ has a very limited freedom in adjustment. Five parameters in Eq. (2), of which only three are fully adjustable, describe the range of the increase in $\lambda_{cm}$ and determine the stress–strain behavior above the inflection point while being of much less importance for the low-strain behavior. Tests of the fitting procedure do not reveal any signs of instability.

## 3. The stress–strain behavior of chemical PVA gels

As mentioned in Section 1, the presence of entanglements is associated with tube-like constraints which hinder the fluctuation of chain segments and create an additional term in the free energy of deformation and in stress. The results obtained in various tube theories [4–10] can be presented in a generalized form [11] and the combination of the Arruda–Boyce connectivity term with the constraint term gives – for systems with zero compressibility – the stress in the form of an equation that we denote by the ABGI code [19]:

$$\sigma_i = 2C_1 \frac{1 - (\lambda_c/\lambda_{cm})^2/3}{1 - (\lambda_c/\lambda_{cm})^2}\left(\lambda_i^2 - \lambda_3^2\right)\Big/\lambda_i + 2C_2\frac{2}{n}\left(\lambda_i^n - \lambda_3^n\right)/\lambda_i \tag{3}$$

The resulting stress–stretch ratio relations in uniaxial extension, equibiaxial extension and in pure shear, together with the expressions for $\lambda_c$, are given in Appendix A. The ABGI equation was shown to give a very good description of the stress–strain behavior of prestrained networks up to high stretch ratios (up to break) [19]. In virgin networks, the strain-induced growth in the finite extensibility parameter $\lambda_{cm}$ is practically always operative and the ABGI equation has to be applied in combination with Eq. (2). We denote such combination by the ABGIL code [19].

The constraint contribution to the modulus is often denoted by $G_e$ in tube theories; the symbol is replaced here with $2C_2$. It is proportional to $d_o^{-2}$, where $d_o$ is the tube radius (mean fluctuation radius of the segment) in the undeformed state [5,12]. The parameter $n$ reflects the constraint mechanism considered in different tube theories which predict values: $-1$ [4], $\langle -1,0\rangle$ [5], 0.5 [6], ~0.45 [7,8], $+1$ [9,10], while the phenomenological Mooney–Rivlin theory [24,25] leads to $n = -2$. In our published articles [13,16,19] and also in studies not published so far, we find, for various systems, the $n$ values mostly in the range from 0 to $+1$. Such result agrees best with the prediction of Gaylord and Douglas [9,10]. Using scaling arguments to account for the global connectivity and local entanglement effects, these authors developed an expression for the free energy which also holds for chains between close parallel plates and for chains strongly adsorbed on a surface. Thus, the expression should also apply to networks containing filler particles and the constraint modulus can be expected to increase with the polymer–filler interfacial area. The expression derived by Gaylord and Douglas contains parameter $\beta$; the use of a space-filling tube model with a constant tube volume deformation condition gives $\beta = -1/2$. A comparison of the Gaylord–Douglas result with the constraint part of Eq. (3) gives $n = -2\beta$; for $\beta = -1/2$, $n = +1$. If the constant tube volume requirement is not imposed on the model, other values of $\beta$ (and $n$) are possible. Gaylord and Douglas admit the possibility that $n$ is not universal for all the network structures and recommend that $n$ be treated as an empirical parameter by fitting the equation to data for a variety of network systems, each under several constant volume deformation conditions [9]. We have followed their recommendation.

The ratio $R_{constr}$ of principal pure shear stresses predicted by the constraint term is given by:

$$R_{constr} \equiv \frac{\sigma_1}{\sigma_2} = \frac{\lambda_1^n - \lambda_1^{-n}}{\lambda_1\left(1 - \lambda_1^{-n}\right)} \equiv \lambda_1^{n-1} + \lambda_1^{-1} \tag{4}$$

$R_{constr}$ is plotted vs the stretch ratio in longitudinal pure shear in Fig. 2 for several values of the parameter $n$. For $n = 2$, the prediction of Eq. (4) is equivalent to that of the Gaussian theory and of the Arruda–Boyce equation (Eq. (1)), i.e., of the connectivity term ($R_{connect}$) of the ABGI equation (Eq. (3)):

$$R_{connect} \equiv \frac{\sigma_1}{\sigma_2} = \frac{\lambda_1^2 - \lambda_1^{-2}}{\lambda_1\left(1 - \lambda_1^{-2}\right)} \equiv \lambda_1 + \lambda_1^{-1} \tag{5}$$

According to Eq. (5), the ratio $R_{connect}$ predicted by the Arruda–Boyce equation monotonically *increases* with $\lambda_1$ and does not depend on the network-chain length. In this respect it differs from that calculated from the Wang and Guth treatment [3] based on a three-chain network model [2] and predicting that for shorter network chains the stress ratio should increase more steeply. Urayama et al. used this theoretical expectation to interpret their experimental data on the physical PVA gels [1].

For $n \le 1.0$, $R_{constr}$ calculated from Eq. (4) monotonically *decreases*. For the Mooney–Rivlin value $n = -2$, $R_{constr}$ is predicted to assume, in the range of $\lambda_1 > 1.42$, values smaller than unity which, however, are physically unrealistic; such prediction disqualifies the Mooney–Rivlin equation [24,25] from application to general deformation modes. For values of $n$ increasing from $-2$ to zero, such limitation is decreasingly restrictive. For networks obeying the ABGIL equation, the stress ratio is predicted to assume values lying

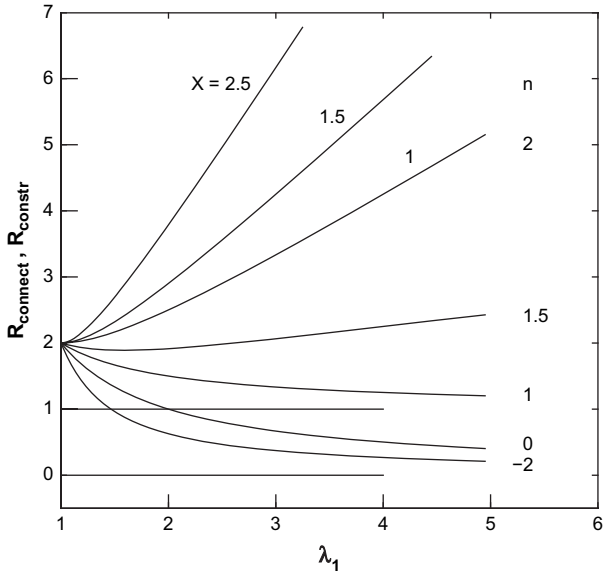


**Fig. 2.** Dependences of the ratio $\sigma_1/\sigma_2$ of principal pure shear stresses on the longitudinal stretch ratio $\lambda_1$. $R_{connect}$ was calculated from Eq. (7) with $X$ increasing from 1 to 2.5, $R_{constr}$ was calculated from Eq. (4) with $n$ decreasing from $+2$ to $-2$.

in the region between $R_{connect}$ and $R_{constr}$ and to depend on $C_2/C_1$ and on the finite extensibility parameter.

The experimental stress–strain data obtained by Urayama et al. on the chemical gel C10 (containing 10 wt% of chemically cross-linked PVA, see Fig. 2 in Ref. [1]) are plotted in Fig. 3 in the coordinates logarithm of reduced stress vs stretch ratio; definitions of reduced stresses are given in Appendix A. In the commonly used stress–strain plots, the absolute values of the differences between the experimental and theoretically calculated stresses become optically very small at low strains even though the relative deviations may be substantial; conversely, at high strains the absolute values of the differences are excessively accentuated. The logarithm of reduced stress has the advantage of showing the relative experiment–theory differences in the whole range of strain with a similar sensitivity.

The growth, with stretch ratio, of experimental reduced stresses in UE and in PS1 (high-strain hardening) which is shown in Fig. 3 indicates a significant contribution of the finite extensibility to the stress. The pure shear data are compared with curves 1 and 2 which are drawn according to the ABGIL equation; their fit to PS1 and PS2 stresses is very good. The relevant parameter values obtained by curve-fitting are given in Table 2. Using the same parameter values, the ABGIL curves 3 and 4 calculated for UE and EBE, respectively, are also drawn. Their fit to the experimental data is less satisfactory and the possible reasons are discussed later on. The $n$ parameter is practically equivalent to the Gaylord–Douglas prediction of unity; the ratio $C_2/C_1 = 1.47$ is rather high.

In Fig. 4, the dependences of the experimental ratio $R$ of the principal pure shear stresses on the stretch ratio are plotted and

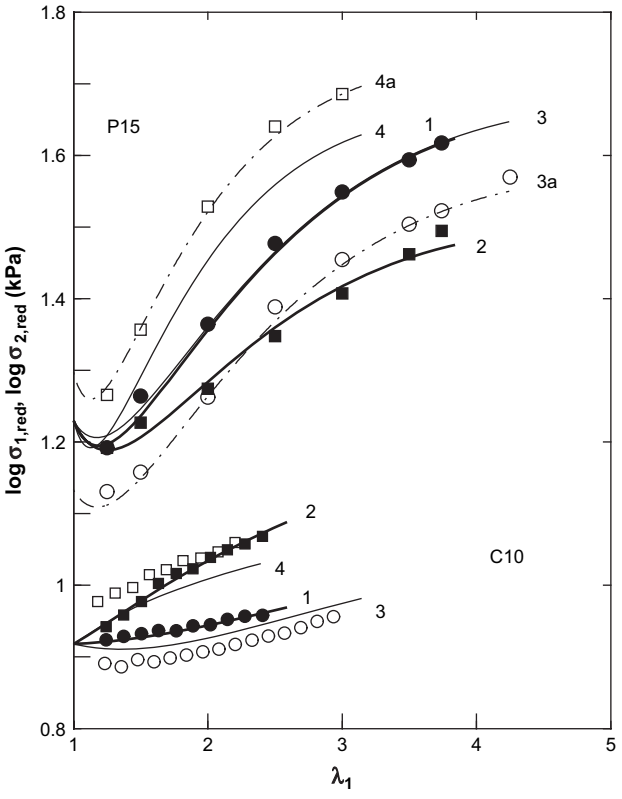


**Fig. 3.** Stretch ratio dependences of the logarithm of reduced stresses for the PVA gels C10 and P15. Experimental data (points) are calculated from the stress–strain data taken from Ref. [1, Figs. 1 and 2]. Curves 1–4, are drawn according to the ABGIL and ABGILFIL equations for parameter values given in Table 2. PS1 – full circles, curves 1; PS2 – full squares, curves 2; UE – open circles, curves 3; EBE – open squares, curves 4. Curves 3a and 4a, were obtained by vertical shifts of curves 3 (−0.0969) and 4 (+0.0676), respectively.

**Table 2**
Parameters of the ABGIL and ABGILFIL equations for the chemical and physical PVA gels

| Parameter | C10 | P15 |
|---|---|---|
| $n$ | 0.9 | 1.0 |
| $2C_1$ (kPa) | 2.36 | 4.2 |
| $2C_2$ (kPa) | 3.46 | 0.8 |
| $\lambda_{c,a}$ | 1.0 | 1.0 |
| $\lambda_{cm,a}$ | 1.28 | 1.25 |
| $\lambda_{c,b}$ | $1.75_8$ | $3.30_9$ |
| $\lambda_{cm,b}$ | 2.01 | $3.50_7$ |
| $a$ | $1.04_5$ | 1.05 |
| $X$ | – | 1.7 |
| $\sigma_{1,red,\lambda_1=1}$ | 8.28 | $16.9_6$ |

compared with the curves drawn according to the ABGIL equation using parameters given in Table 2. The fit to the data on the chemical gel C10 is very good and substantiates the explanation of the observed approximate constancy of $R$ in chemical gels: with increasing stretch ratio and for $n \leq 1.0$, $R_{constr}$ decreases below 2 and this effect obviously compensates the increasing trend of $R_{connect}$ predicted for the connectivity term.

Measurements of Urayama et al. show that for the gel C7.5 with a lower PVA concentration, the values of the experimental $R$ (Fig. 4, full circles) are somewhat smaller than those of the C10 gel (full squares). In the absence of detailed data on C7.5, one can but envisage the theoretically possible reasons for such behavior; one of them is a decrease in $n$. A curve is drawn through the C7.5 points with $n$ decreased from 0.9 to 0.3 and its fit to the data is good. The remaining parameters were kept unchanged but this is a rather crude approximation. In our previous paper [16] we found that in a series of poly(dimethylsiloxane) networks endlinked in the presence of an inert diluent, the parameters $n$, $C_1$, $C_2$, $C_2/C_1$ had a tendency to decrease with increasing diluent concentration; changes in the finite extensibility parameter can be assumed to occur too.

Urayama et al. measured stresses in different deformation modes at very low stretch ratios ($\lambda_1 < 1.1$) and evaluated the slopes of the stress–strain dependences (see Table 1 in Ref. [1]). Assuming

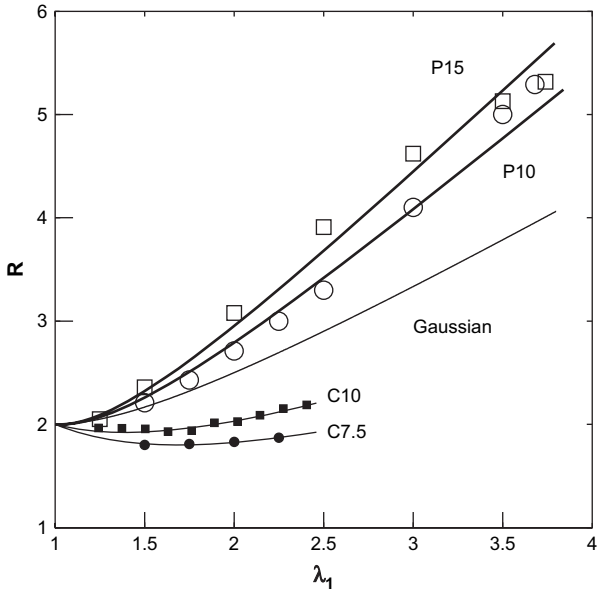


**Fig. 4.** Dependences of the ratio $R = \sigma_1/\sigma_2$ of the principal pure shear stresses on the longitudinal stretch ratio $\lambda_1$ for the physical and chemical PVA gels. Experimental points are calculated from stresses given in Figs. 1 and 2 in Ref. [1]. Curves are drawn according to the ABGIL and ABGILFIL equations for parameter values given in Table 2; for C7.5, $n = 0.3$; for P10, $X = 1.5$. The Gaussian curve is drawn according to Eq. (5).

zero compressibility, one can calculate the respective $G$ moduli for the different deformation modes. It is found for the C10 network that the experimental EBE modulus is somewhat higher (+3%) and the UE modulus somewhat lower (−3%) than the longitudinal pure shear modulus. Urayama ascribed the effect to an experimental error and to a non-zero compressibility.

In the semilogarithmic plot in Fig. 3, the experimental dependences in all the four geometrical modes should theoretically extrapolate to the same value at unit stretch ratio. However, this is not the case. The extrapolated zero-strain logarithm of reduced stress in UE is by some 0.018 (4%) lower and that in EBE by approx. 0.0365 (8.7%) higher than the respective values in pure shear. The factors 1.04 and 1.087 are but slightly higher than those ($\approx 1.03$) found by Urayama et al. [1, Table 1]. If compressibility is zero, then this effect should be due to some kind of experimental scatter (e.g., crosslinking degrees of the samples used for UE, EBE and PS measurements may not be the same). The differences +0.018 and −0.0365 between the respective experimental UE and EBE data and the UE and EBE curves 3 and 4 (based on fitted pure shear curves) are almost independent of strain, the experimental-to-calculated stress ratio being given by strain-independent multiplicative factors, respectively.

All the four curves and the experimental points given in Fig. 3 for the chemical PVA gel are replotted in Fig. 5 in linear coordinates. The dashed lines for UE and EBE are calculated using the parameter values based on pure shear data (Table 2). The stresses given by full lines 3 and 4 were obtained by multiplying the corresponding dashed line stresses using factors based on the Urayama measurements of the low-strain moduli. The factor for the UE full line 3 was 1/1.03, and that for the EBE full line 4 was 1.03. The full lines so obtained describe the data with a satisfactory accuracy, thus giving a reasonable support to the ABGIL approach.

## 4. The stress–strain behavior of physical PVA gels

In the following, the physical PVA gels are looked upon as two-phase networks with the soft rubbery phase formed by water-diluted polymer chains and with the hard phase formed by microcrystallites, which play a simultaneous role of multifunctional crosslinks and of inextensible domains amplifying the local strain in the rubbery phase. In agreement with the Urayama reasoning [1], one can expect that in physical gels the concentration of trapped entanglements and, consequently, the topological constraint contribution to the stress will be much smaller than in chemical PVA gels. On the other hand, one should take into account that, in the presence of hard microcrystalline domains, the required macroscopic (external) strain, $\varepsilon_i$, is achieved with the microscopic (internal) strain in the elastomer matrix, $\varepsilon_{i,\mathrm{int}}$, being higher than $\varepsilon_i$; this will give rise to a strain-amplification factor $X$ [4,12]:

$$X = \varepsilon_{i,\mathrm{int}}/\varepsilon_i; \tag{6}$$

$$\lambda_{i,\mathrm{int}} = 1 + \varepsilon_{i,\mathrm{int}} = 1 + X\varepsilon_i \tag{6a}$$

The internal (microscopic) stretch ratio is amplified to $\lambda_{i,\mathrm{int}} = 1 + X\varepsilon_i$ and this quantity should be introduced into Eqs. (3) and (1a) for $\lambda_i$ to calculate the quantities $I_{1,\mathrm{int}}$ and $\lambda_{c,\mathrm{int}}$, which are then used to obtain the macroscopic stress observed at a macroscopic (external) strain $\varepsilon_i$ (at an external stretch ratio $\lambda_i = 1 + \varepsilon_i$). The information on $X$ is obtained from stress–strain measurements [4,12,13], i.e., $X$ is treated as an adjustable parameter. For the combination of Eqs. (2), (3), and (6a) we use the code ABGILFIL [13].

For $C_2 = 0$ and constant values of $X$ higher than unity, the dependences of $R$ on the macroscopic stretch ratio $\lambda_1$ predicted by the ABGILFIL equation are obtained from Eq. (5) using the internal stretch ratio:

$$R_{\mathrm{connect}} = \lambda_{1,\mathrm{int}} + 1/\lambda_{1,\mathrm{int}}$$

$$R_{\mathrm{connect}} = 1 + X(\lambda_1 - 1) + [1 + X(\lambda_1 - 1)]^{-1} \tag{7}$$

The curves calculated from Eq. (7) are plotted in Fig. 2. With increasing $X$, the overall slope of the $R_{\mathrm{connect}}$ vs $\lambda_1$ dependence increases while no effect of the network-chain length is predicted. The experimental observation of Urayama et al. that for physical PVA gels the ratio $R$ of principal pure shear stresses is higher than that calculated by the Gaussian theory [1] using macroscopic stretch ratios

$$\frac{\sigma_1}{\sigma_2} > \lambda_1 + \lambda_1^{-1} \tag{8}$$

is thus predicted by the ABGILFIL equation to be due to the amplification of local strain in the presence of hard-phase particles, providing that $C_2/C_1$ is zero or small.

Using definitions of reduced stresses given in Appendix A and a simple algebraic manipulation, Eq. (8) can be rearranged to

$$\sigma_{1,\mathrm{red}} > \sigma_{2,\mathrm{red}} \tag{9}$$

which gives another relation characterizing the pure shear behavior of physical PVA gels; for the gel P15 it is shown in Fig. 3. In the same graph the inverse behavior $\sigma_{1,\mathrm{red}} < \sigma_{2,\mathrm{red}}$ of the chemical gel C10 is shown; it corresponds to that of common polymer networks (conf. Refs. [13,16,19]).

The dependences of the logarithm of reduced principal pure shear stresses (Fig. 3, P15, curves 1 and 2) and of the ratio $R$ of principal pure shear stresses (Fig. 4) on the stretch ratio are described by the ABGILFIL equation reasonably well; the fitted parameter values are given in Table 2. The steeply increasing trend of the reduced stress in PS1 is due both to the effect of a low finite extensibility and to the strain-amplification factor being higher than unity.

For the physical gel P12, the ratio $R$ increases less steeply than that for the P15 gel (Fig. 4). In the first approximation, this effect was ascribed here to the lower value of the amplification factor (1.5 vs 1.7). A decrease in the strain-amplification factor with increasing dilution is a reasonable expectation. In the absence of more detailed

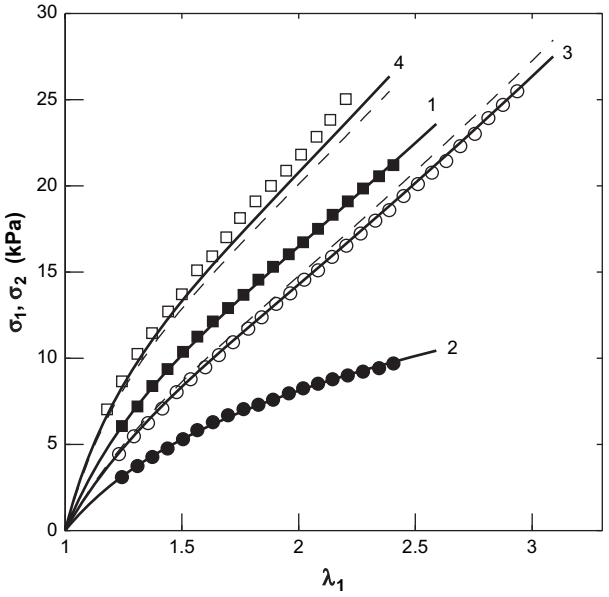


**Fig. 5.** Comparison of the experimental stress–stretch ratio dependences of the chemical PVA gel C10 (points) with the ABGIL equation; parameters in Table 2. Full lines: 1 – PS1, 2 – PS2; dashed lines: 3 – UE, 4 – EBE. Full lines 3 and 4 are corrected by factors based on low-strain moduli and on the assumption of zero compressibility.

experimental data, the effect of the remaining parameters cannot be estimated and the same values are used as found for P15.

Similar to the behavior of the chemical gel C10 (Figs. 3 and 5), the experimental stresses (Fig. 6) and the corresponding reduced stresses (Fig. 3) in UE and EBE of the physical gel P15 differ from the respective curves 3 and 4 calculated using the parameter values obtained by fitting the ABGILFIL equation to pure shear data. For the physical gel, however, the differences are significant and the shifts of the calculated curves 3 and 4 required for a satisfactory description of the respective experimental reduced stresses (curves 3a and 4a in Fig. 3) are large: −0.0969 for UE and +0.0675 for EBE. The extrapolations of the experimental dependences of reduced stresses in UE and EBE, respectively, to zero strain give significantly lower (higher) reduced stresses at unit stretch ratio than the values calculated on the basis of pure shear measurements. This observation leaves open questions regarding, on the one side, the ability of the ABGILFIL equation to predict the UE and EBE behaviors from pure shear measurements and, on the second side, the reliability of the experimental measurements. One point is worth mentioning. The ratio $R_{up}$ = sUE/sPS1 of the stresses in uniaxial extension and longitudinal pure shear calculated from data on common rubber networks [17,18,26–29] and shown in Fig. 7 increases with stretch ratio $\lambda_1$ from the initial theoretical value 0.75 [1] to ~0.87 at $\lambda_1 \approx 2$; for natural and isoprene rubber networks values of $\lambda_1 > 3$ can be achieved with $R_{up}$ tending from 0.95 to unity. The $R_{up}$ points of the chemical gel C10 lie in the group of points of common crosslinked rubbers. On the other hand, the physical gel P15 shows a completely different behavior, its $R_{up}$ being significantly lower in the whole range of strain: at low stretch ratios it starts somewhere below 0.75, then it increases but even at $\lambda_1 \approx 3.5$ it does not exceed 0.77. Since the ratio of the transverse-to-longitudinal stress in shear (sPS2/sPS1) determined by Urayama for P15 is lower than that for C10, one would rather expect its sUE to be closer to sPS1 (i.e., its $R_{up}$ to be closer to unity) than is observed for C10. Further experimental study might help to answer these questions.

## 5. Deformation energy $W$ as a function of invariants $I_1$, $I_2$

Urayama et al. analyzed the behavior of chemical and physical PVA gels in terms of the deformation energy $W(I_1,I_2)$ expressed as

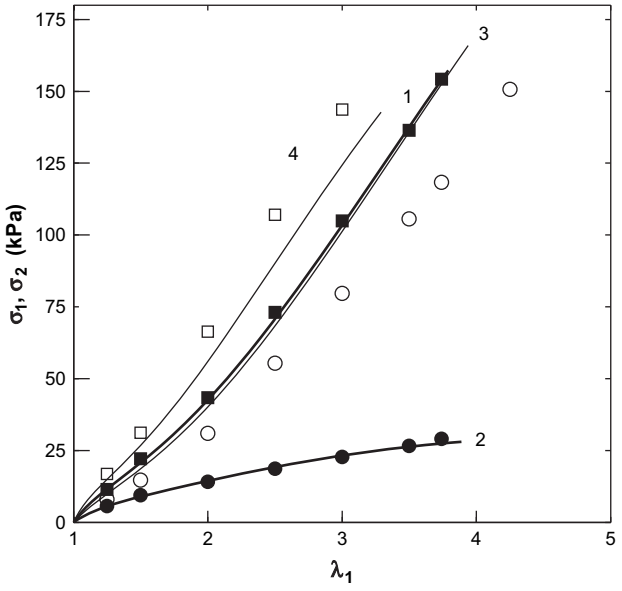


**Fig. 6.** Comparison of the experimental stress–stretch ratio dependences of the physical PVA gel P15 (points) with curves calculated according to the ABGILFIL equation (parameters in Table 2 are based on pure shear data). PS1 – full squares, curve 1; PS2 – full circles, curve 2; UE – open circles, curve 3; EBE – open squares, curve 4.

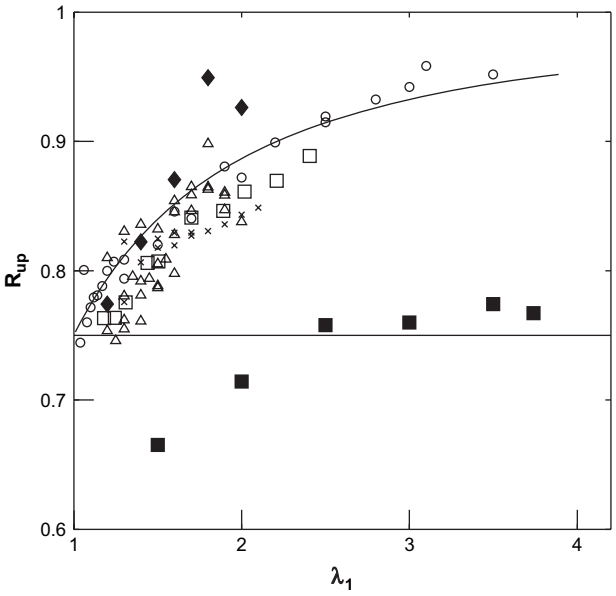


**Fig. 7.** Dependence of $R_{up}$ = sUE/sPS1 on stretch ratio for the following networks: crosses – SBR [26], open triangles – PDMS [27,28], open circles – IR [29], NR [17], full diamonds – NR + HAF carbon black [18], open squares – C10, full squares – P15. Curve: calculated for the NR network [17] using the ABGIL parameters determined in Ref. [19].

a function of the first and second invariants of the deformation tensor, $I_1 = \sum_i \lambda_i^2$ (see Eq. (1a)) and $I_2 = \sum_i 1/\lambda_i^2$, zero compressibility was assumed [1]. The derivatives of $W(I_1,I_2)$ with respect to $I_1$ and $I_2$ are denoted by the symbols $W_1$ and $W_2$, respectively. For pure shear deformation ($\lambda_2 = 1$) the derivatives read:

$$W_1 = \frac{1}{2\left(\lambda_1^2 - 1\right)}\left(\frac{\lambda_1^3\sigma_1}{\lambda_1^2 - \lambda_1^{-2}} - \frac{\sigma_2}{1 - \lambda_1^{-2}}\right) \tag{10a}$$

$$W_2 = \frac{-1}{2\left(\lambda_1^2 - 1\right)}\left(\frac{\lambda_1\sigma_1}{\lambda_1^2 - \lambda_1^{-2}} - \frac{\sigma_2}{1 - \lambda_1^{-2}}\right) \tag{10b}$$

Urayama et al. calculated the values of the derivatives from their experimental data and showed that for chemical PVA gels both $W_1$ and $W_2$ are positive and little dependent on the stretch ratio. For the physical gels, $W_1$ is positive and increases with stretch ratio, while $W_2$ is negative in practically the whole range of deformations; as articulated by Urayama et al., this is the first observation for elastomers. For both chemical and physical gels, $W_1$ and $W_2$ in the small strain limit exhibit upswing and downswing, respectively; this has often been observed for various elastomers, as discussed by Urayama et al. [1].

Using definitions of reduced stresses, Eqs. (10a) and (10b) can also be expressed as follows:

$$W_1 = \frac{1}{2\left(\lambda_1^2 - 1\right)}\left(\lambda_1^2\sigma_{1,\mathrm{red}} - \sigma_{2,\mathrm{red}}\right) \tag{11a}$$

$$W_2 = \frac{-1}{2\left(\lambda_1^2 - 1\right)}\left(\sigma_{1,\mathrm{red}} - \sigma_{2,\mathrm{red}}\right) \tag{11b}$$

If $(\sigma_{1,\mathrm{red}} - \sigma_{2,\mathrm{red}})$ is positive, as found for the physical gels, then according to Eq. (11b) $W_2$ must be negative, and *vice versa*. The dependences of $W_1$ and $W_2$ on the invariant $I_1$ (= $I_2$) that we have calculated from the Urayama stress–strain measurements (points in Figs. 8 and 9) can be described by the ABGILFIL equation (curves) very well using the parameter values given in Table 2.

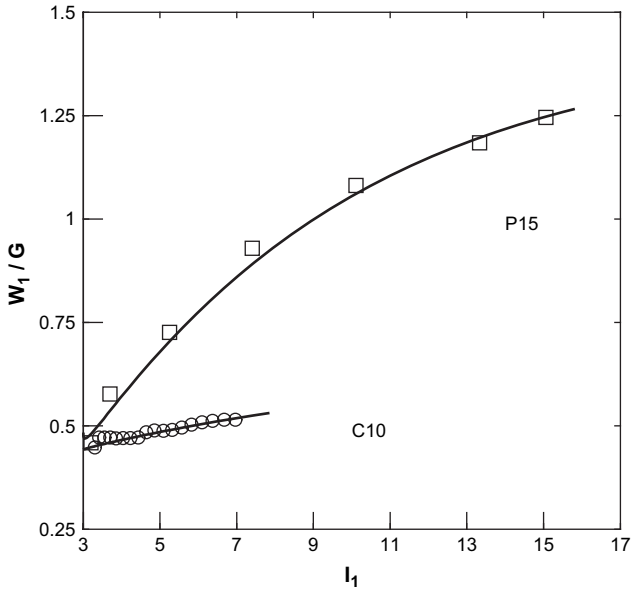


**Fig. 8.** The derivatives $W_1$ (reduced by the respective initial moduli given in Table 2) as functions of $I_1$. Points: calculated from the experimental stresses, Eq. (10a). Curves: drawn according to the ABGILFIL equation using parameters given in Table 2.

Urayama et al. suppose that the characteristics of the physical PVA gels originate from the structural features such as fewer amounts of slippery-trapped entanglements along network strands compared with the chemical PVA gels. In agreement with this argument is the low value of $C_2$ that we found for the physical gel P15. This factor alone, however, cannot explain the observations $R > (\lambda_1 + 1/\lambda_1)$; $\sigma_{1,\mathrm{red}} > \sigma_{2,\mathrm{red}}$; $W_2 < 0$. Although the Wang and Guth equation [3] predicts that $R$ should be larger than $(\lambda_1 + 1/\lambda_1)$, it fails in the crucial respect: it is not able to describe the behavior of PVA gels in different deformation modes, as was already concluded by Urayama et al. [1].

The comparison of the Urayama experimental data with the ABGILFIL equation leads to the following conclusions:

The stress–strain behavior in pure shear of physical PVA gels is in agreement with its two-phase structure where microcrystalline

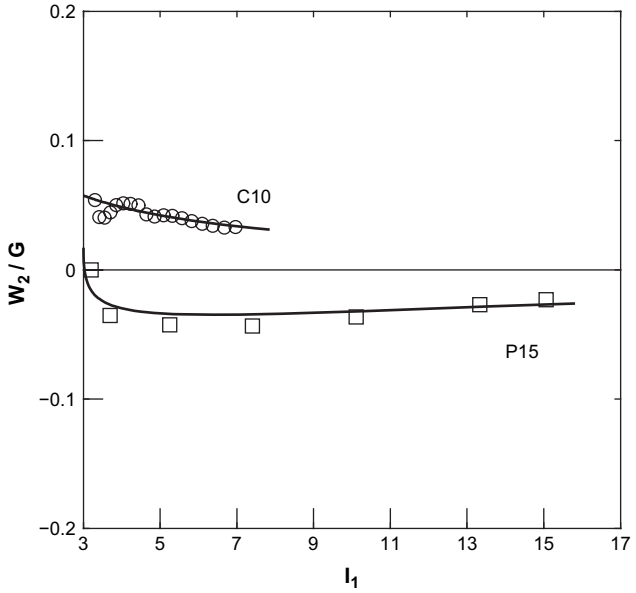


**Fig. 9.** The derivatives $W_2$ (reduced by the respective initial moduli given in Table 2) as functions of $I_1$. Points: calculated from the experimental stresses, Eq. (10b). Curves: drawn according to the ABGILFIL equation using parameters given in Table 2.

**Table 3**
Contributions to the reduced stress at zero strain $\sigma_{1,\mathrm{red},\lambda_1=1}$

| Contributions to $\sigma_{1,\mathrm{red},\lambda_1=1}$ | NC (kPa) | *NC* (%) | C10 (kPa) | *C10* (%) | P15 (kPa) | *P15* (%) |
|---|---|---|---|---|---|---|
| Network chains (Gaussian)[a] | 0.85 | *99.4* | 2.36 | *28.5* | 4.2 | *24.8* |
| Finite extensibility[b] | 0.005 | *0.6* | 2.46 | *29.7* | 4.98 | *29.4* |
| Topological constraints[c] | – | – | 3.46 | *41.8* | 0.8 | *4.7* |
| Strain amplification by crystallites[d] | – | – | – | – | 6.98 | *41.1* |
| $\sigma_{1,\mathrm{red},\lambda_1=1}$ | 0.855 | *100* | 8.28 | *100* | 16.96 | *100* |

$\sigma_{1,\mathrm{red},\lambda_1=1} = (2C_1 + \mathrm{FE} + 2C_2)X$.
[a] $2C_1$: stress held by network chains in the Gaussian limit.
[b] $\mathrm{FE} = (\sigma_{1,\mathrm{red},\lambda_1=1}/X) - 2C_1 - 2C_2$.
[c] $2C_2$.
[d] $(2C_1 + \mathrm{FE} + 2C_2)(X - 1)$.

inextensible domains amplify the local strain (increase the strain amplifier $X$ above unity) and this leads to the growth in the overall slope of the $R$ vs $\lambda_1$ dependence, to a decrease in $\sigma_{2,\mathrm{red}}$ below $\sigma_{1,\mathrm{red}}$ and to a decrease in $W_2$ below zero. The low degree of entanglement results in a constraint modulus $C_2$ that is low and, thus, it has little effect on the overall slope of the $R$ vs $\lambda_1$ dependence. It should be noted that in filler-reinforced networks the presence of filler amplifies the local strain but at the same time it enhances tube-like constraints thereby reducing $R$. For instance, from the James and Green measurements [18] on a prestrained natural rubber vulcanizate reinforced with carbon black, we arrived at the parameter values $X = 1.9$, $C_2/C_1 \approx 0.5$, $\sigma_{1,\mathrm{red}} \approx \sigma_{2,\mathrm{red}}$, $W_2 \approx 0$ [13].

## 6. Conclusions

(1) The hydrogel based on poly(*N*,*N*-dimethylacrylamide) cross-linked with nanoplatelets of a synthetic Mg–Li–Na silicate (Table 3, NC) behaves at low and medium elongations according to the Arruda–Boyce equation; at high elongations it shows deviations which can be ascribed to a strain-induced increase in the finite extensibility parameter. Such deviations are typical of all the virgin rubbery networks that we have studied so far [13,16,19].

(2) The stress–strain behavior (in UE, EBE, PS) of chemical PVA gels and the pure shear behavior of physical PVA gels can be satisfactorily described by the constitutive ABGILFIL equation which comprises the following contributions:
   (A) Langevin-statistics-based equation derived in the Arruda and Boyce theory [14];
   (B) Strain-induced increase in the finite extensibility parameter which takes place on the first extension of virgin networks [13,16,19];
   (C) The Gaylord–Douglas theory of topological constraints [9,10];
   (D) The amplification of local strain in the presence of inextensible particles [4,12] (fillers, crystalline or glassy domains).

The numerical values of the four contributions to the reduced stress at zero strain are shown for the three networks in Table 3. Low-strain contributions imparted by network chains and by finite extensibility have similar relative values for the chemical gel C10 and the physical gel P15. The contribution of topological constraints is large in C10 and small in P15 while that of strain amplification by crystallites is large in P15 and zero in C10.

(3) The Urayama stress–strain measurements on the chemical gel C10 in the four geometrical modes, pure shear measurements on the chemical gel C7.5 and on the physical gels P15 and P12 are described by the ABGILFIL constitutive equation in

a reasonably good manner. The prediction of the UE and EBE behavior of the physical gel P15 from pure shear measurements leaves some open questions; further experimental study might help to answer them. The observations $R > (\lambda_1 + 1/\lambda_1)$, $\sigma_{1,\mathrm{red}} > \sigma_{2,\mathrm{red}}$, $W_2 < 0$ found for physical gels is quantitatively explained by amplification of local strain due to the presence of crystallites. In physical gels, this effect is not counteracted by topological constraints, which are small here, possibly due to a low degree of network-chain entanglement. The ratio $R$ almost independent of strain found in chemical gels results from the compensation of the opposing effects imparted by the connectivity and constraint terms.

## Acknowledgement

The authors are greatly indebted to the Grant Agency of Academy of Sciences of the Czech Republic for financial support within the grant project No. IAA-400500701.

## Appendix A

Stress–strain relations (Eq. (3)) can be written in the general form

$$\sigma_i = A_1\left(\lambda_i^2 - \lambda_3^2\right)\Big/\lambda_i + A_2(\lambda_i^n - \lambda_3^n)/\lambda_i \tag{A1}$$

The meaning of $A_1$, $A_2$ follows from a comparison of Eq. (A1) with Eq. (3).

Special cases of Eq. (A1) for the most often used geometrical modes are the following.

Stress in uniaxial extension UE

$$\lambda_3 = \lambda_2 = 1/\lambda_1^{1/2};\ \lambda_c = \left\{\left(\lambda_1^2 + 2/\lambda_1\right)\Big/3\right\}^{1/2}$$

$$\sigma_1 = A_1\left(\lambda_1 - 1/\lambda_1^2\right) + A_2\left(\lambda_1^{n-1} - 1/\lambda_1^{(1+n/2)}\right);\ \sigma_2 = 0; \tag{A2}$$

Stress in equibiaxial extension EBE

$$\lambda_1 = \lambda_2;\ \lambda_c = \left\{\left(2\lambda_1^2 + 1/\lambda_1^4\right)\Big/3\right\}^{1/2}$$

$$\sigma_1 = A_1\left(\lambda_1 - 1/\lambda_1^5\right) + A_2\left(\lambda_1^{n-1} - 1/\lambda_1^{(1+2n)}\right);\ \sigma_2 = \sigma_1 \tag{A3}$$

Stresses in pure shear PS

$$\lambda_2 = 1;\ \lambda_3 = 1/\lambda_1;\ \lambda_c = \left\{\left(\lambda_1^2 + 1 + 1/\lambda_1^2\right)\Big/3\right\}^{1/2}$$

longitudinal pure shear stress sPS1

$$\sigma_1 = A_1\left(\lambda_1 - 1/\lambda_1^3\right) + A_2\left(\lambda_1^{n-1} - 1/\lambda_1^{(1+n)}\right) \tag{A4}$$

transverse pure shear stress sPS2

$$\sigma_2 = A_1\left(1 - 1/\lambda_1^2\right) + A_2\left(1 - 1/\lambda_1^n\right) \tag{A5}$$

Reduced stresses are defined as the ratios of stress and of the corresponding Gaussian stretch ratio function.

Reduced stress in uniaxial extension $\sigma_{\mathrm{red,UE}} = \sigma_{\mathrm{UE}}/(\lambda_1 - 1/\lambda_1^2)$.
Reduced stress in equibiaxial extension $\sigma_{\mathrm{red,EBE}} = \sigma_{\mathrm{EBE}}/(\lambda_1 - 1/\lambda_1^5)$.
Reduced stress in longitudinal pure shear $\sigma_{\mathrm{red,PS1}} = \sigma_{\mathrm{PS1}}/(\lambda_1 - 1/\lambda_1^3)$.
Reduced stress in transverse pure shear $\sigma_{\mathrm{red,PS2}} = \sigma_{\mathrm{PS2}}/(1 - 1/\lambda_1^2)$.

## References

[1] Urayama K, Ogasawara S, Takigawa T. Polymer 2006;47:6868–73.
[2] James HM, Guth E. J Chem Phys 1943;11:455–81.
[3] Wang MC, Guth E. J Chem Phys 1952;20:1144–57.
[4] Klüppel M, Schramm J. Macromol Theory Simul 2000;9:742–54.
[5] Kaliske M, Heinrich G. Rubber Chem Technol 1999;72:602–32.
[6] Heinrich G, Straube E. Acta Polym 1983;34:589–94.
[7] Rubinstein M, Panyukov S. Macromolecules 1997;30:8036–44.
[8] Rubinstein M, Panyukov S. Macromolecules 2002;35:6670–86.
[9] Gaylord RJ, Douglas JF. Polym Bull 1987;18:347–54.
[10] Gaylord RJ, Douglas JF. Polym Bull 1990;23:529–33.
[11] Heinrich G, Straube E, Helmis G. Adv Polym Sci 1988;85:33–87.
[12] Luo H, Klüppel M, Schneider H. Macromolecules 2004;37:8000–9.
[13] Meissner B, Matějka L. Polymer 2006;47:7997–8012.
[14] Arruda EM, Boyce MC. J Mech Phys Solids 1993;41:389–412.
[15] Cohen A. Rheol Acta 1991;30:270–3.
[16] Meissner B, Matějka L. Polymer 2004;45:7247–60.
[17] James AG, Green A, Simpson GM. J Appl Polym Sci 1975;19:2033–58.
[18] James AG, Green A. J Appl Polym Sci 1975;19:2319–30.
[19] Meissner B, Matějka L. Polymer 2003;44:4599–610.
[20] Wu PD, van der Giessen E. Mech Phys Solids 1993;41:427–56.
[21] Haraguchi K, Farnworth R, Ohbayashi A, Takehisa T. Macromolecules 2003;36:5732–41.
[22] Haraguchi K, Takehisa T, Fan S. Macromolecules 2002;35:10162–71.
[23] Haraguchi K, Li HJ, Takehisa T, Elliot E. Macromolecules 2005;38:3482–90.
[24] Mooney M. J Appl Phys 1940;11:582–92.
[25] Rivlin RS. Philos Trans R Soc London Ser A 1948;241:379–97.
[26] Arenz RJ. J Appl Polym Sci 1977;21:2453–63.
[27] Kawamura T, Urayama K, Kohjiya S. Macromolecules 2001;24:8252–60.
[28] Kawamura T, Urayama K, Kohjiya S. J Polym Sci Part B Polym Phys 2002;40:2780–90.
[29] Kawabata S, Matsuda M, Kawai H. Macromolecules 1981;14:154–62.